Electron bombardment of water adsorbed on Zr(0001) surfaces

2003 J. Phys.: Condens. Matter 15 1899

(http://iopscience.iop.org/0953-8984/15/12/307)

INSTITUTE OF PHYSICS PUBLISHING JOURNAL OF PHYSICS: CONDENSED MATTER

J. Phys.: Condens. Matter **15** (2003) 1899–1908 PII: S0953-8984(03)55741-1

Electron bombardment of water adsorbed on Zr(0001) surfaces

S Ankrah[1], Y C Kang[1,2] and R D Ramsier[1,2,3,4]

[1] Department of Physics, The University of Akron, Akron, OH 44325-4001, USA
[2] Department of Chemistry, The University of Akron, Akron, OH 44325-4001, USA
[3] Department of Chemical Engineering, The University of Akron, Akron, OH 44325-4001, USA

E-mail: rex@uakron.edu

Received 7 November 2002
Published 17 March 2003
Online at stacks.iop.org/JPhysCM/15/1899

Abstract

A study of the effects of electron bombardment on water adsorbed on Zr(0001) is reported. Zirconium surfaces are dosed with isotopic water mixtures at 160 K followed by electron bombardment (485 eV). The system is then probed by low energy electron diffraction, temperature programmed desorption (TPD) and Auger electron spectroscopy (AES). No evidence is found that would indicate preferential mixing of hydrogen from the bulk with isotopic water dissociation products during TPD. However, electron bombardment results in the sharpening of a hydrogen/deuterium desorption peak near 320 K and the production of water near 730 K at low water exposures. In addition, although water does not oxidize Zr(0001) thermally, electron bombardment of adsorbed water induces a shift of about 2 eV in the Zr AES features indicating that the surface is partially oxidized by electron bombardment.

1. Introduction

A major use of zirconium and its alloys in the nuclear community is for cladding uranium oxide fuel. It is well suited for this purpose because it is corrosion resistant and does not readily absorb thermal neutrons [1]. In such applications, Zr is in contact with chemical compounds like water and heavy water (D_2O) under severe temperatures and pressures in a radiation environment. It is the behaviour of the surface of the material under these conditions that will inevitably result in corrosion propagation or mitigation. It is our goal here to address such processes from a model-system standpoint, and in particular the possibility of initiating surface chemistry by electron bombardment.

Apart from thermal activation, surface processes such as chemisorption, migration, desorption and diffusion can be stimulated by electronic excitation using photon, electron or

[4] Author to whom any correspondence should be addressed.

ion/neutral bombardment. In such circumstances, we can initiate processes which are thermally inaccessible [2–8]. Energetic species may be ejected from the surface as a result of electronic excitation or may participate in surface chemistry that is not thermally accessible. The use of electron-beam methods for controlled modification of surface species is of practical importance in many materials systems. In this paper, we discuss the effects of electron bombardment on isotopic water adsorbed on Zr(0001) surfaces. After electron bombardment, we probe the system with temperature programmed desorption (TPD), low energy electron diffraction (LEED) and Auger electron spectroscopy (AES).

2. Experimental details

Detailed information and a schematic diagram of the ultra-high vacuum (UHV) system used in this study (base pressure $\sim 1.3 \times 10^{-8}$ Pa) have previously been presented [9]. The Zr(0001) cylindrical single crystal is 1 mm thick and 6 mm in diameter. This substrate (Mateck Material-Technologie & Kristalle GmbH) has a purity of 99.99% but no dislocation density or chemical analysis data is available. One side is mechanically polished to a surface roughness of 3×10^{-8} m with an accuracy of orientation better than 1° along the $\langle 0001 \rangle$ axis. Tantalum wires are spot welded to the sides of the crystal, which are then mounted on to machined copper arms. Two type-E thermocouples are spot welded to opposite sides of the single crystal and the assembly is mounted on a manipulator that allows for motion along three orthogonal axes and rotation about the manipulator axis. A copper braid connects a liquid-nitrogen-cooled cold finger to one of the copper arms for sample cooling and power leads connected to the copper arms provide resistive heating.

A quadrupole mass spectrometer (QMS) is used for TPD experiments, which are performed with a temperature ramp of 1.6 K s^{-1}. The QMS is multiplexed to record the partial pressures of H_2O (18 amu), HDO (19 amu), D_2O (20 amu), H_2 (2 amu), HD (3 amu) and D_2 (4 amu). The 18 amu signal is a combination of $H_2O^+ + \alpha\{D_2O^+\}$ signals, where α is the OD^+/D_2O^+ cracking fragment ratio. We use this and the measured 19 and 20 amu signals to calculate the actual $D_2O/HDO/H_2O$ ratios from the raw data. Hydrogen exchange can occur in the gas handling system even though high purity D_2O is used and there is also residual H_2O in the vacuum system that must be accounted for in determining total water exposures. The QMS monitors the partial pressures of these species during backfilling and the integrated areas of these dosing curves are used to determine total water exposure. This also allows us to check for isotope-dependent desorption kinetics.

Using an electron flood gun, the Zr(0001) surface is bombarded with electrons (485 eV) for different times before TPD experiments are performed. The zirconium surface is cleaned by sputtering with Ar^+ (2 keV, 0.02 A m^{-2}) in two-hour cycles followed by annealing at 840 K for 2 min. Sharp (1 × 1) LEED patterns (60 eV, 0.02 A m^{-2}) characteristic of Zr(0001) are observed and collected using a digital camera before TPD experiments are performed. Deuterium oxide (D_2O 99.9% purity, Aldrich) and argon (99.9999% purity, Matheson) are connected to the reactive and inert sections, respectively, of a stainless steel gas handling system. Water exposure is carried out by backfilling the chamber through a precision leak valve and exposures are reported in Langmuir (L) units (1 L $= 1.3 \times 10^{-4}$ Pa s). Uncertainties in total exposure are assumed to be on the order of 0.2 L. AES data (3 keV, 0.15 A m^{-2}) are taken at 160 K following stepwise annealing. Our cleaning procedure leaves some oxygen and carbon detectable by AES, but the carbon is considered non-reactive since we do not observe significant CO or CO_2 production in TPD.

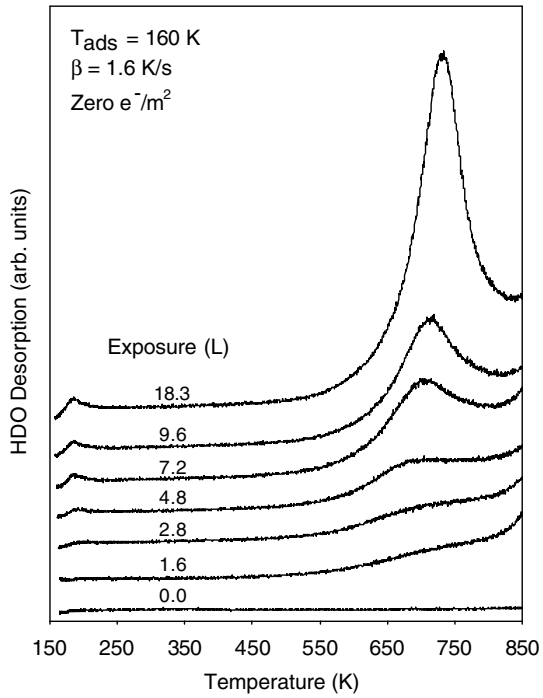

Figure 1. Representative TPD spectra of HDO (19 amu) from Zr(0001) following 160 K adsorption of isotopic water at various exposures without electron bombardment.

3. Results

3.1. Temperature programmed desorption

During TPD experiments, we use the QMS to measure partial pressures of possible compounds containing hydrogen, oxygen and deuterium atoms. The main products desorbing from Zr(0001) following water exposure and heating are D_2, D_2O, HD, HDO, H_2 and H_2O, with or without electron bombardment. As the exposure increases at 160 K, TPD features of H_2O, HDO and D_2O near 730 K begin to develop. Figure 1 shows such a series of HDO spectra without electron bombardment, taken in random order to minimize systematic error. Note the 730 K peak profile development, the low temperature (about 175 K) feature and the exposure range. Comparing these data to figure 2, taken after water adsorption and electron bombardment, three things are clear. The low temperature feature is absent, the high temperature peak profile is the same, and the development of this peak occurs at about the same water exposures. It should be noted that figures 1 and 2 are plotted on the same vertical scale, and that very little water desorbs at low exposures in both cases. We do not know the exact nature of the species responsible for the sloping high temperature backgrounds. This could result from the diffusion and surface recombination of species from the bulk, or be attributable to desorption from other regions of the sample holder. It should be noted here that the isotopic ratios of the thermally desorbing species do not change with electron bombardment, and we therefore have no evidence of isotope effects.

We also observe changes in hydrogen desorption spectra with electron bombardment. Figure 3 represents TPD spectra of D_2 from Zr(0001) after isotopic water exposure at 160 K. Broad features at about 320 K do not change with increasing exposure. Note that these features

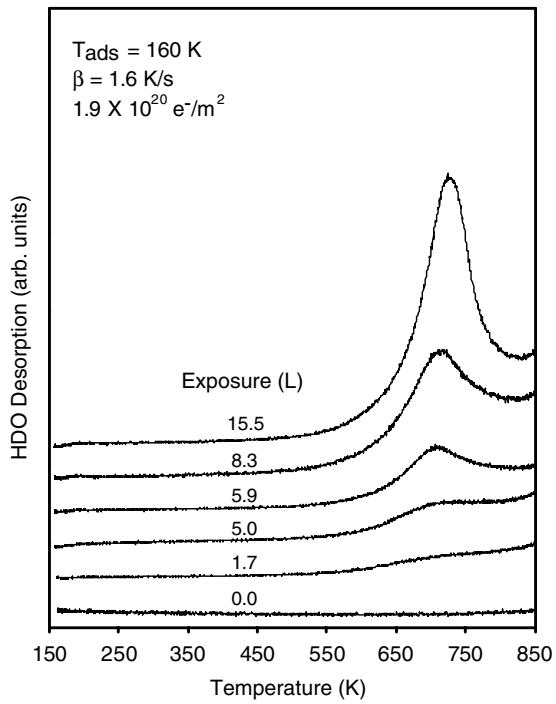

Figure 2. Representative TPD spectra of HDO (19 amu) from Zr(0001) following 160 K adsorption of isotopic water at various exposures with electron bombardment (beam energy = 485 eV).

are not concomitant with water desorption, unlike the 730 K feature which is due to a QMS fragment of the water desorbing at high temperature. Figure 4 shows TPD spectra of D_2 from Zr(0001) following electron bombardment (1.9×10^{20} e^- m^{-2}) of adsorbed water at 160 K, with the same vertical scale as figure 3. There is a sharp D_2 desorption peak developing near 320 K and the broad low temperature structure is diminished as compared to figure 3. This implies that electron bombardment selectively removes some of the hydrogen/deuterium from the surface, either by inducing desorption or dissolution, resulting in a narrower thermal desorption feature with lower overall yield. Another possibility might be that we stimulate the production of hydrocarbons that would consume some of the surface hydrogen; however, we do not detect species such as CH_4^+ during TPD. TPD is also performed at constant water exposure and varying electron fluence (from $1.9–225 \times 10^{20}$ e^- m^{-2}), but there is no noticeable electron fluence dependence in this range. These data (not shown) indicate that the effect of electron bombardment saturates at a fluence less than 2×10^{20} e^- m^{-2}, consistent with the known sensitivity of water and its thermal dissociation products (hydrogen and hydroxyl species) to electron induced effects [2]. Most importantly, these fluence studies demonstrate that potential heating effects due to the flood gun beam are not responsible for the changes in TPD and AES spectra (discussed below).

3.2. Auger electron spectroscopy and low energy electron diffraction

Figure 5 presents AES spectra of water adsorbed on Zr(0001), focusing on the Zr features. It can be seen that there is a shift of about 2 eV in the Zr(MNV) feature after electron bombardment and slight heating, implying that Zr is oxidized by +1 [10–13]. This is caused by electron

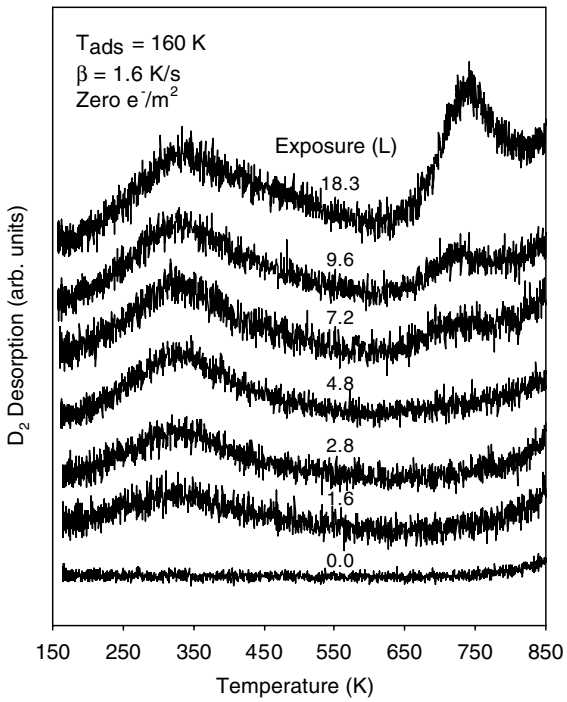

Figure 3. Representative TPD spectra of D_2 (4 amu) from Zr(0001) following 160 K adsorption of isotopic water at various exposures without electron bombardment.

bombardment since water does not oxidize Zr(0001) thermally under these conditions. Note that after water desorption, the remaining oxygen does not dissolve into the substrate until annealing temperatures reach 850 K. This is also evident in figure 6, which shows representative O(KLL)/Zr(MNV) peak-to-peak height ratios taken from AES spectra. After water exposure (in this data-set 7.9 L), there is an increase in the O(KLL)/Zr(MNV) ratio indicating an increase in oxygen concentration on the surface as expected. However, after electron bombardment of adsorbed water, there is a further increase in the O(KLL)/Zr(MNV) ratio. These changes occur at about 160 K, and show that electron bombardment results in an appreciable increase in oxygen content near the surface (figure 6) and a modification of the surface oxidation state (figure 5).

Data from LEED (not shown) indicate that the adsorption of water on Zr(0001) at 160 K does not result in ordered overlayers, but annealing to 710 K results in a (2×2) pattern. Residual oxygen from the dissociation of water and from the subsurface region is responsible for these patterns. A sharp (1×1) pattern can be obtained by annealing to 850 K, and we have no evidence that oxygen ordering is induced by electron bombardment. The LEED observations are consistent with those of AES and indicate that residual oxygen dissolves into the substrate during annealing to 850 K, probably residing in the region just beneath the surface. We have previously shown with isotopic oxygen that subsurface species are kinetically mobile, chemically active, and participate in surface reactions [14].

4. Discussion

It is known that energetic species may be ejected from metal surfaces as a result of electronic excitation. These species, which are often fragments of the parent-adsorbed molecule, may

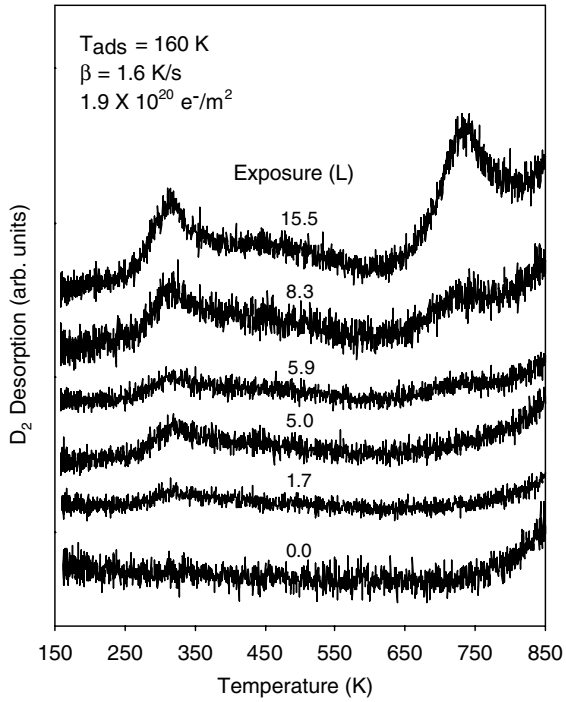

Figure 4. Representative TPD spectra of D_2 (4 amu) from Zr(0001) following 160 K adsorption of isotopic water at various exposures with electron bombardment (beam energy = 485 eV).

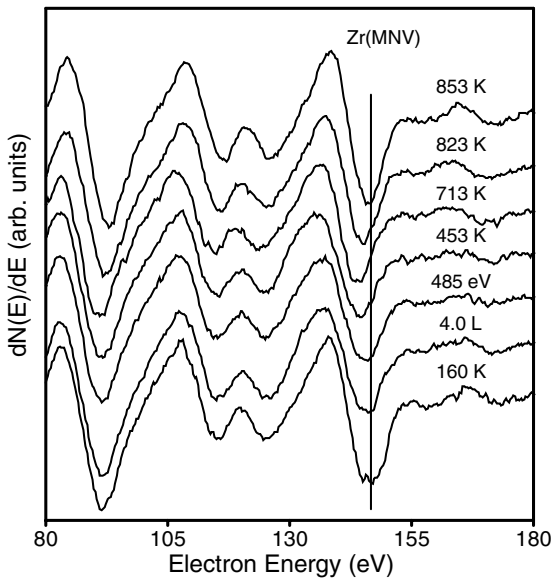

Figure 5. Auger electron spectra taken after stepwise annealing where the vertical line is to focus attention on the Zr(MNV) Auger features. The bottom three spectra represent the surface before water exposure, after 4.0 L water exposure and after 485 eV electron bombardment, all at 160 K.

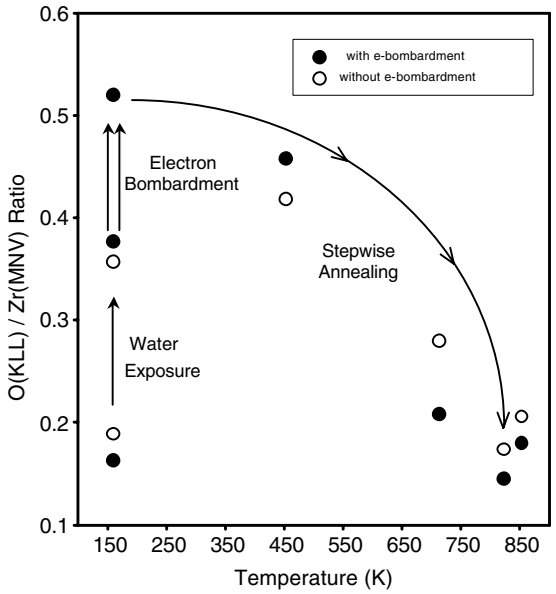

Figure 6. AES O(KLL)/Zr(MNV) peak-to-peak height ratios taken before water exposure, after water exposure (7.9 L), after electron bombardment, and after stepwise annealing.

also be captured on the surface. The low energy density of the soft electron beam does not result in significant substrate heating, and we attribute changes in our TPD and AES spectra to electronic excitation effects. We make this assignment based on the fact that there is no significant temperature rise of the sample during electron bombardment even at very high fluence. The electrons probably initiate hydrogen and deuterium electron stimulated desorption (ESD) [15–20], which alters the low temperature thermal desorption features near 320 K by depleting the adsorbed H/D and OH/OD species known to exist on this surface at these temperatures [21, 22]. This sharpens up the 320 K hydrogen feature, possibly due to selective ESD depletion of either one type of species or of the same species at different binding sites. Hydroxyl species are known to be thermally stable until about 200 K on this surface, so we consider them as likely candidates for electron induced decomposition under our conditions. It is also possible that electron bombardment stimulates the dissolution of hydrogen and deuterium into the metal.

The excitation process can also form electronically excited oxygen atoms which do not escape the surface. These radical oxygen atoms then partially oxidize the Zr(0001) surface, similar to processes involving ultraviolet light and ozone [23]. This partially oxidized surface layer is stable during AES, accounting for the increased O/Zr ratios seen after electron bombardment, but dissociates at higher temperatures. The shifts of about 2 eV seen in the Zr(MNV) AES features after electron bombardment indicate that the oxidation state of Zr changes by +1 [10–13]. Water adsorption does not oxidize Zr(0001) thermally under the present conditions, and we therefore conclude that the oxygen produced as a result of electron bombardment is responsible for surface oxidation. This again argues that hydroxyls are dissociated by electron induced processes.

We propose one possible reaction scheme below, where the letters A–G, I and J are stoichiometric coefficients and H stands for hydrogen and deuterium. The letters in parentheses indicate gas phase (g), adsorbed phase (a) and subsurface phase (s). Adsorption at 160 K

follows

$$A\{H_2O(g)\} \rightarrow A\{H(a)\} + A\{OH(a)\} \tag{1}$$

and temperature ramping results in

$$\begin{aligned} A\{H(a)\} + A\{OH(a)\} \rightarrow\ & B\{H_2O(g)\}(175\ K) + \\ & C\{H_2(g)\}(175\text{–}475\ K) + \\ & D\{H_2O(g)\}(550\text{–}850\ K) + \\ & E\{O(s)\}(850\ K) \end{aligned} \tag{2}$$

where A = B + C + D to conserve the number of hydrogen atoms and A = B + D + E for the oxygen atoms, or in other words C = E. Our TPD control spectra (0.0 water exposure) and mass balance imply that conservation should hold for both O and H species, and we know from AES that we have residual oxygen in the subsurface region. This oxygen can dissolve into the bulk and enter a solid solution phase or desorb during high temperature annealing in the cleaning cycles.

Electron (e) bombardment at 160 K modifies the kinetics as follows, assuming complete destruction of the surface hydroxyl species and no oxygen ESD, for simplicity.

$$A\{H(a)\} + A\{OH(a)\} + e \rightarrow A\{O^*(a)\} + F\{H^*(g)\} + G\{H(a)\} + e \tag{3}$$

where the symbol (*) stands for electronically excited and A = F + G. We also see from our AES data (figures 5 and 6) that O* binds with Zr, represented in what follows by the sub-oxide Zr_2O. Temperature ramping now yields

$$\begin{aligned} A\{Zr_2O\} + G\{H(a)\} \rightarrow\ & I\{H_2(g)\}(250\text{–}350\ K) + \\ & J\{H_2O(g)\}(550\text{–}850\ K) + \\ & E\{O(s)\}(850\ K) + \\ & 2A\{Zr\}(850\ K) \end{aligned} \tag{4}$$

where G = 2(I + J) and A = J + E. Note that our model predicts the amount of residual oxygen to be these same (E) in both schemes, consistent with figure 6. Also note that the latter scheme has no low temperature water desorption, consistent with figure 2. Combining the mass balance relationships we have J + E = B + D + E which implies J > D with non-zero B, or that more water desorbs thermally at high temperature following electron bombardment with the same low temperature water exposure (compare figures 1 and 2). We can also form the combination J + C = 2I + 2J + F, which indicates that C > I, or that more hydrogen desorbs at low temperature in the absence of electron bombardment (compare figures 3 and 4). Thus we have a proposed scheme that is self-consistent and accounts for most of our observations.

We should mention that we work in the 160–180 K [9] adsorption temperature range because it is convenient experimentally and we know that water adsorption kinetics are complicated here [21, 22]. Li *et al* [22] reported an ice layer desorbing at 163 K and a second layer at 178 K, following 80 K water adsorption on Zr(0001). The first chemisorbed layer produced no low temperature water desorption, and they also report deuterium thermal desorption near 320 K. Adsorption at 158 K allowed them to observe the second layer desorbing in TPD without ice formation. The data reported here for 160 K adsorption show a low temperature feature that is easily removed by electron bombardment, presumably corresponding to the second layer described by Li *et al* [22]. However, our cleaning and annealing procedure is such that we always have some subsurface oxygen present and we are working in very high water exposure regimes, so direct comparisons are not possible.

Finally, we need to explain why low fluences of 485 eV electrons cause an increase in the O/Zr AES ratios as shown in figure 6. One might reason that if low energy electrons

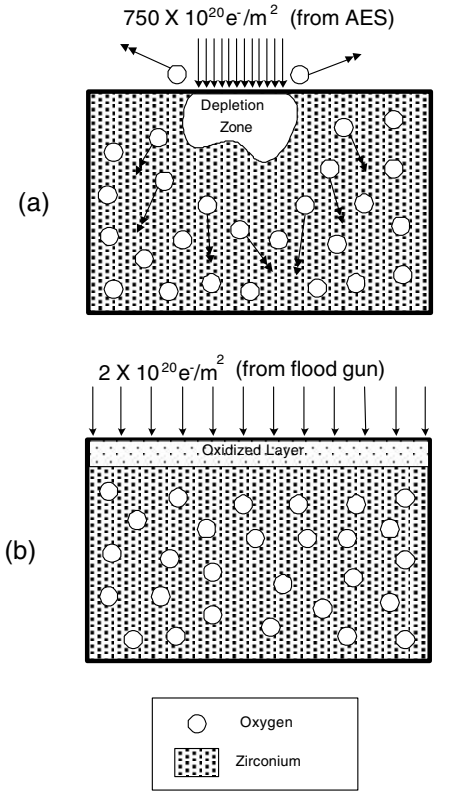

Figure 7. Conceptual model depicting the case without/with electron bombardment. (a) Without electron bombardment the AES beam causes oxygen to diffuse into the substrate or desorb from the surface. (b) With electron bombardment a partially oxidized surface layer forms which is subsequently stable during AES.

can cause O*(a) production and trapping at the surface, then the 3 keV electrons we use for AES should cause the same effect. With this reasoning, we should always measure a partially oxidized surface and a larger O/Zr ratio in AES experiments, with or without low energy electron bombardment. However, this is not the case. Figure 7 presents a conceptual model to explain our interpretation of why the AES electron gun does not cause the same effects as the flood gun.

Figure 7(a) depicts what happens in the case without soft electron bombardment. Electrons from AES have a relatively high energy (3 keV) and fluence (about 750×10^{20} e^- m^{-2}) and are highly focused in a small spot. This causes a local temperature gradient that causes oxygen to diffuse away and an oxygen depletion zone is formed. We measure sample temperature rises on the order of 20 K during AES, with constant sample cooling, so our temperature gradient model is reasonable. Since the AES electrons have energies greater than the O(1s) binding energy, it is also probable that ESD mechanisms further deplete the surface oxygen content, also depicted in the illustration. Figure 7(b) summarizes the case involving electron bombardment. Here we imply that the low energy electrons do not make a significant temperature gradient, at least not laterally. They also do not cause oxygen ESD to a large extent, but instead aid in the trapping of oxygen on the surface and the formation of a partially oxidized layer. The layer is stable overall with respect to subsequent electrons from the AES beam, but dissolves at high

temperatures to liberate water and leave residual oxygen in the subsurface region. We do not show hydrogen species in figure 7 in the interest of clarity, which should undergo ESD in both cases.

5. Summary

In this study, the interaction of soft electrons with isotopic water adsorbed on Zr(0001) is investigated by TPD, LEED and AES. It is known that Zr(0001) is very reactive with respect to water and other small molecules, and we find evidence that soft electron bombardment can be used to modify the resulting thermal kinetics. We propose a reasonable mechanism based on the electron induced decomposition of surface hydroxyls. This removes H species and leaves electronically excited O atoms at the surface which bind to Zr atoms to form a sub-oxide. We observe changes in TPD and AES spectra consistent with our proposed scheme. Thus we have indications, at least from a model system standpoint with a simulated radiation environment, that zirconium surface reactions can differ in the presence of electronic excitation from those stimulated thermally.

Acknowledgments

Acknowledgement is made to the Donors of the American Chemical Society Petroleum Research Fund for partial support of this research. Partial support of this work by the Research Corporation is also acknowledged.

References

[1] Cox B 2000 *Uhlig's Corrosion Handbook* 2nd edn (New York: Wiley) ch 49
[2] Ramsier R D and Yates J T Jr 1991 *Surf. Sci. Rep.* **12** 243
[3] Popova I, Zhukov V and Yates J T Jr 1999 *Appl. Phys. Lett.* **75** 3108
[4] Ebinger H D and Yates J T Jr 1998 *Surf. Sci.* **412/413** 1
[5] Lu Q-B and Madey T E 2000 *Surf. Sci.* **451** 238
[6] Romberg R, Frigo S P, Ogurtsov A, Feulner P and Menzel D 2000 *Surf. Sci.* **451** 116
[7] Bater C, Sanders M and Craig J H Jr 2000 *Surf. Interface Anal.* **29** 188
[8] Bater C, Campbell J H and Craig J H Jr 1998 *Surf. Interface Anal.* **26** 97
[9] Kang Y C, Milovancev M M, Clauss D A, Lange M A and Ramsier R D 2000 *J. Nucl. Mater.* **281** 57
[10] Tanabe T and Tomita M 1989 *Surf. Sci.* **222** 84
[11] Zhang C-S, Flinn B J and Norton P R 1992 *Surf. Sci.* **264** 1
[12] Nishino Y, Krauss A R, Lin Y and Gruen D M 1996 *J. Nucl. Mater.* **228** 346
[13] Tomita M, Tanabe T and Imoto S 1989 *Surf. Sci.* **209** 173
[14] Kang Y C and Ramsier R D 2002 *Appl. Surf. Sci.* **195** 196
[15] Ojima K and Ueda K 2000 *Appl. Surf. Sci.* **165** 149
[16] Simpson W C, Wang W K, Yarmoff J A and Orlando T M 1999 *Surf. Sci.* **423** 225
[17] Ojima K and Ueda K 2000 *Appl. Surf. Sci.* **165** 141
[18] Hoflund G B, Asbury D A and Gilbert R E 1987 *J. Vac. Sci. Technol.* A **5** 1124
[19] Asbury D A, Hoflund G B, Peterson W J, Gilbert R E and Outlaw R A 1987 *Surf. Sci.* **185** 221
[20] Davidson M R, Hoflund G B and Outlaw R A 1993 *Surf. Sci.* **281** 213
[21] Li B, Griffiths K, Zhang C-S and Norton P R 1997 *Surf. Sci.* **384** 70
[22] Li B, Griffiths K, Zhang C-S and Norton P R 1997 *Surf. Sci.* **370** 97
[23] Ramanathan S, Wilk G D, Muller D A, Park C-M and McIntyre P C 2001 *Appl. Phys. Lett.* **79** 2621